Fluorescence Based Structural Analysis of Tryptophan Analogue-AMP Formation in Single Tryptophan Mutants of *Bacillus stearothermophilus* Tryptophanyl-tRNA Synthetase†

Mauro Acchione,‡ Joseph G. Guillemette,§ Susan M. Twine,‡ Christopher W. V. Hogue,|| Bahe Rajendran,⊥ and Arthur G. Szabo*,‡

Wilfrid Laurier University, Waterloo, Canada N2L 3C5

Received May 7, 2003; Revised Manuscript Received September 18, 2003

ABSTRACT: The symmetrical dimer structure of tryptophanyl-tRNA synthetase is similar to that of tyrosyl-tRNA synthetase whose binding behavior and structural details have been elucidated in detail. The structure of both subunits after forming the intermediate tryptophanyl-AMP has important implications for the binding of the cognate $tRNA^{Trp}$. Single tryptophan mutants of *Bacillus stearothermophilus* tryptophanyl-tRNA synthetase have been constructed and expressed and used to probe structural changes in different domains of the enzyme in both subunits. Substrate titrations using the Trp analogues 4-fluorotryptophan and 7-azatryptophan in the presence of ATP to form the corresponding aminoacyl-adenylate reveal significant structural changes occurring throughout the active subunit in regions not confined to the active site. Changes in environment around the specific Trp residues were monitored using UV absorbance and steady-state fluorescence measurements. When titrated with 4-fluorotryptophan, both Trp 91 and Trp 290 fluorescence is quenched (49 and 22%, respectively) when one subunit has formed Trp-AMP. The fluorescence of Trp 48 is enhanced 19%. No further change in signal was observed after a 1:1 dimer/L-4FW-AMP complex ratio had been established. Using an anion-exchange filter binding assay with radiolabeled L-Trp as a substrate, binding to only one subunit was observed under nonsaturating conditions. This agrees with the results of the assay using 7-azatryptohan as a substrate. The observed changes extend to the unfilled subunit where a similar structure is believed to form after one subunit has formed tryptophan-AMP. Movement in the regions of the enzyme containing Trp 290 and Trp 91 suggests a mechanism for cross-subunit communication involving the helical backbone and dimer interface containing these two residues.

Tryptophanyl-tRNA synthetase (TrpRS[1] will be used to denote the wild-type protein) is a member of a unique family of essential enzymes that have a role in maintaining the fidelity of the genetic code (*1*, *2*). Aminoacyl-tRNA synthetases (aaRSs) catalyze the charging of tRNA with its cognate amino acid in two steps (Scheme 1), the first being the activation of the enzyme-bound amino acid by adenosine triphosphate (ATP) to form a high-energy aminoacyl-adenosine monophosphate (AMP) intermediate. Binding of the cognate tRNA to the enzyme then results in transfer of the amino acid via esterification to the 3′ end of the tRNA.

Scheme 1: Two-Step Reaction Mechanism for TrpRS

1) Trp + ATP + TrpRS ⇄ TrpRS (Trp-AMP) + PPi

2) TrpRS (Trp-AMP) + $tRNA^{Trp}$ ⇄ TrpRS + $tRNA^{Trp}$ (Trp) + AMP

This group of 20 ubiquitous enzymes has been extensively investigated (*2*−*5*). Much of this interest is motivated by the varying substrate specificities (*2*−*4*), differences in substrate binding mechanism (*6*−*8*), potential as targets for anti-viral agents (*9*), and more recently, the identification of noncanonical functions (*10*). The aaRSs also exhibit differences in both size and oligomerization. These include monomers, dimers (α_2, $\alpha\beta$), and tetramers (α_4, $\alpha_2\beta_2$) (*2*). Among prokaryotes, such as *Escherichia coli* and *Bacillus subtilis*, 10 synthetases have been identified as functional dimers (*2*). Generally, it has been found that this dimeric structure is a prerequisite for catalytic activity in these enzymes. TrpRS is a homodimer, and both subunits are capable of forming the Trp-AMP intermediate and charging the cognate $tRNA^{Trp}$ (*11*−*13*). From fluorescence measurements and analysis of the X-ray crystal structure, the TrpRS dimer shows a high degree of symmetry when both subunits are filled with Trp-AMP (*14*). A recent structure of the substrate-free form of this enzyme revealed some asymmetry in the segments that bind Trp (*15*). Previous work on TrpRS isolated from bovine pancreas suggested nonequivalence in structure between the two subunits when one Trp-AMP is

† Funding for this work was provided by a grant from the Natural Sciences and Engineering Research Council of Canada.

* To whom correspondence should be addressed. Tel: (519) 884-0710 ext. 2401. E-mail: aszabo@wlu.ca.

‡ Department of Chemistry, Wilfrid Laurier University, Waterloo, Canada N2L 3C5.

§ Department of Chemistry, University of Waterloo, Waterloo, Canada N2L 3G1.

|| Samuel Lunenfeld Institute, Mount Sinai Hospital, Toronto, Canada, M5G 1X5.

⊥ Department of Chemistry and Biochemistry, University of Windsor, Windsor, Canada M9B 3P4.

[1] Abbreviations: TrpRS, tryptophanyl-tRNA synthetase; aaRSs, aminoacyl-tRNA synthetases; ATP, adenosine triphosphate; AMP, adenosine monophosphate; TyrRS, tyrosyl-tRNA synthetase; GlnRS, glutaminyl-tRNA synthetase; SerRS, seryl-tRNA synthetase; 4FW, 4-fluorotryptophan; 7AW, 7-azatryptophan; PPiase, inorganic pyrophosphatase.

10.1021/bi0347454 CCC: $25.00
Published on Web 11/21/2003

bound (*16*). For tyrosyl-tRNA synthetase (TyrRS), the X-ray crystal structure of the dimer is symmetrical, but in solution, there is a half-of-sites reactivity observed for $tRNA^{Tyr}$ substrate (*17*) that can be rationalized by the binding of one $tRNA^{Tyr}$ molecule across both subunits as shown in the X-ray crystal structure. The structure for *Bacillus stearothermophilus* TrpRS suggests a similar (analogous to *E. coli* TyrRS) two-subunit tRNA binding mechanism. The predicted site of $tRNA^{Trp}$ activation is too close to the amino acid binding site for proper positioning of $tRNA^{Trp}$ on one subunit (*14*). An important question raised by this proposed two-subunit tRNA binding mechanism is the structure and active site occupancy of both subunits prior to tRNA binding. For the much larger *E. coli* glutaminyl-tRNA synthetase (GlnRS), the symmetrical dimer can function as two independent subunits, each capable of charging a separate $tRNA^{Gln}$ molecule simultaneously (*18*). Seryl-tRNA synthetase (SerRS) also functions as a dimer, and the bound $tRNA^{Ser}$ makes contact with both subunits (*19*).

Affinity for the various substrates and substrate analogues, the order of their binding, and the activity of each subunit in the dimer are often dissimilar even for the same aaRSs from different species (*18*). *E. coli* TrpRS shows no preference for the initial binding of either Trp or ATP, has positive cooperativity toward Trp binding, and displays half-of-sites reactivity (*20*). TrpRS from bovine pancreas also displays a random order to ATP and $tRNA^{Trp}$ binding but displays an apparent anti-cooperativity toward Trp binding (*16*). There is, however, some disagreement over this since it has been suggested that the observed anti-cooperativity is due to inhibition by bound inorganic pyrophosphate (PPi). Anti-cooperativity was not observed in the presence of $tRNA^{Trp}$ or PPiase (*21*). There are examples indicating that both subunits of the dimer can form the active intermediate and that such a 2:1 complex is stable (*14*, *22*). However, in terms of $tRNA^{Trp}$ charging, all TrpRS show half-of-sites reactivity (i.e., only one tRNA charged at a time) when stoichiometric concentrations of substrates are used at physiological temperatures and pH (*16*, *23*). Analysis of sequence mutations in Trp auxotrophic mutants of *E. coli* TrpRS has revealed several residues in the dimer interface that play a role in catalytic efficiency. It has been suggested that these residues serve to properly position the C-terminal helix with respect to the Rossmann fold in the active site (*24*). Trp 92 is located at the dimer interface of *B. subtilis* TrpRS. Mutation of this residue to a tyrosine was also found to abolish activity of the enzyme (*25*). Taken together, these results indicate that several residues other that those required for specific substrate binding are essential for the proper structure and function of the enzyme.

Early experiments using intrinsic protein fluorescence revealed that large structural changes occurred during the course of the aminoacylation reaction in eukaryotic systems (*26*). Titration of bovine TrpRS with Trp in the presence of excess ATP results in the quenching of intrinsic Trp fluorescence. This change reaches a plateau at 2:1 Trp to dimer binding. For *B. subtilis* TrpRS, the fluorescence quenching that was observed upon titration with ATP in the presence of excess Trp plateaus after 1:1 ATP to dimer binding, although it was expected that both active sites were filled under the conditions used (*22*). This was rationalized as a concerted structural change occurring in both subunits after one active site was filled, which implied cross-subunit communication. Further evidence for a structural change occurring in both subunits comes from the magnitude of the fluorescence quenching observed. Since the enzyme is a symmetrical homodimer, the fluorescence contribution of each subunit is expected be equal. Therefore, there cannot be a greater than 50% change in the fluorescence signal if only one subunit is filling and if there were no concerted change in the second substrate-free subunit. This was not what was observed for *B. subtilis* whose Trp fluorescence decreases by 70% (*22*).

Questions regarding this binding mechanism remain. Does the second subunit fill under nonsaturating physiological conditions? Are there regions of the enzyme other than the active site and dimer interface that undergo dynamic movements when forming Trp-AMP, and how may these changes be involved in enzyme function? What structure is presented to the substrates on the second free subunit after the first Trp-AMP has formed? Is it the same structure formed as in the Trp-AMP-bound subunit as shown in the X-ray crystal structure? To further investigate the nature of the structural changes occurring on formation of the Trp-AMP intermediate, single Trp mutants of *B. stearothermophilus* TrpRS have been constructed. *B. stearothermophilus* TrpRS contains the conserved residue (Trp 91) at the dimer interface as well as two others (Trp 48 and Trp 290). Trp 290 is positioned at the end of the helix that forms a long V-shaped backbone to one subunit and inserts into the dimer interface. Trp 48 follows the helix adjacent to the C-terminal end of the Rossmann β-sheet fold in the active site (*14*).

Stoichiometry of Trp-AMP formation and the corresponding structural changes at each Trp position were monitored using steady-state fluorescence. The difficulty in interpreting results from these experiments is that one cannot distinguish changes in fluorescence of the substrate Trp from those that may be occurring in Trp residues located in the protein. Studying single Trp mutants becomes an even greater problem since the substrate Trp now makes a larger contribution to the overall fluorescence signal. To solve this problem, the fluorescent probes 4-fluorotryptophan (4FW) and 7-azatryptophan (7AW) were used as substrate analogues. Both these analogues have been shown to be fully active as substrates for TrpRS (*27*−*29*). These and other Trp analogues confer a number of spectroscopic advantages in protein structure−function studies (*30*). 4FW exhibits negligible fluorescence at the temperatures and excitation wavelength used in this study and therefore permits monitoring of the intrinsic fluorescence of the enzyme without interference from substrate Trp. The fluorescence of 7AW shows a high degree of sensitivity to its local environment, and its absorption profile allows for selective excitation at 310 nm (*31*). We have reported earlier on its use in measuring 7AW-AMP formation in *B. subtilis* TrpRS (*27*). The results presented here are consistent with the induction of a structural change in the unoccupied subunit after one subunit forms the active intermediate. The stoichiometry of Trp-AMP formation, as observed with fluorescence and radioisotope assays, indicates that the second subunit is not occupied (active) under nonsaturating conditions. The possible significance of these results for the binding of substrates will be discussed together with the site-specific correlation of fluorescence results with published X-ray crystal structures.

MATERIALS AND METHODS

Materials. Competent BL21(DE3) *E. coli* cells were obtained from Invitrogen (Burlington, Canada). Glycerol and growth medium for expression from the TrpRS containing vectors were purchased from VWR Canlab (Toronto, Canada) as was the $CaCl_2$ and Na_2HPO_4 used in the synthesis of hydroxyapatite. DEAE Sephacel and Sephacryl S200 HR chromatography media were purchased from Pharmacia Biotech (Piscataway, NJ). L-[5-^{3}H] Trp was obtained from Amersham Biosciences (Piscataway, NJ) as an ethanol/water (1:1) solution with a specific activity of 24 Ci/mmol. L-Tryptophan, the amino acid analogues DL-4FW and DL-7AW, adenosine triphosphate, dithiothreitol, isopropyl β-D-1-thiogalactopyranoside (IPTG), and all additional reagents were purchased from Sigma-Aldrich (St. Louis, MO).

Mutagenesis of B. stearothermophilus TrpRS. The *B. stearothermophilus* TrpRS expression vector was a generous gift from Dr. Dieter Soll of Yale University. It consists of the pETNS1 plasmid composed of the native gene for *B. stearothermophilus* TrpRS subcloned as a NdeI-BamHI fragment into the expression vector pET3a (Novagen, Madison, WI). Mutagenesis was performed by the method of overlap extension mutagenesis (*32*) using the appropriate oligonucleotide primers. The coding region for TrpRS and relevant parts of each of the expression vectors were fully sequenced at the MOBIX facility at McMaster University (Hamilton, Canada) to ensure that no spontaneous mutations had resulted from the polymerase chain reaction used in the mutagenesis procedure. Mutant proteins were generated wherein two of the three tryptophan residues were replaced by a tyrosine. The mutants generated for this report include *B. stearothermophilus* W91Y/W290Y (W48), *B. stearothermophilus* W48Y/W290Y (W91), and *B. stearothermophilus* W48Y/W91Y (W290).

Expression and Purification of TrpRS. Plasmids carrying the TrpRS gene were transformed into BL21(DE3) cells for high level expression and cultured in LB medium supplemented with 2% glycerol at 37 °C with constant shaking until an OD_{600} of 1.0 was reached. Protein expression was induced with IPTG to a final concentration of 1 mM, and cultures were incubated at 37 °C for an additional 4 h before cells were harvested by centrifugation at 4 °C. The purification procedure used has been previously described (*27*). In place of vacuum filtration during the hydroxyapatite batch adsorption step, the mixture was washed twice with 400 mL of 0.1 M K_2HPO_4, 1 mM DTT, 0.5 mM PMSF, 0.5 mM EDTA, pH 6.8 and centrifuged at 3000*g* to recover the hydroxyapatite. The protein was then eluted by agitating gently in 100 mL of 0.5 M K_2HPO_4, 1 mM DTT, 0.5 mM PMSF, 0.5 mM EDTA, pH 6.8 for 10 min at room temperature. The protein was recovered by centrifuging at 3000*g* for 15 min at 4 °C. Residual hydroxyapatite was removed by a final spin at 40 000*g* for 5 min at 4 °C.

Circular Dichroism Measurements. Protein samples were prepared in 10 mM PIPES, 100 mM NaF, pH 7.0 at a final concentration of 2 μM. Elipticity was measured from 195 to 300 nm in a 1 × 1 cm cuvette. Each spectrum was corrected using a buffer blank.

Time-Correlated Single Photon Counting (TCSPC) Measurements. Time-resolved fluorescence parameters for *B. stearothermophilus* TrpRS and single Trp mutants were determined using a frequency doubled argon ion-pumped dye laser (Spectra-Physics, Mountain View, CA). The details of the apparatus used and methods for data analysis have been described in detail previously (*27*, *33*). An excitation wavelength of 295 nm was used, and the fluorescence was recorded at various wavelengths corresponding to the steady-state spectrum.

Substrate Titrations. Samples for substrate titrations monitored using steady-state and time-resolved fluorescence were prepared as follows. Stock solutions of enzyme were prepared from lyophilized protein powder that was resuspended in buffer consisting of 100 mM NaCl, 1 mM DTT, 20 mM Tris-HCl, pH 8.0 (Assay Buffer). Samples were centrifuged at 15 000*g* for 10 min and then applied to a 1 × 15 cm preequilibrated (assay buffer) column of Sephadex G50 to remove aggregates. Protein concentration in eluted fractions was determined with the BCA assay (*34*) using BSA as a standard.

In titrations using 4FW to form 4FW-AMP, an initial reaction volume of 2 mL was used, which contained 1 μM TrpRS, 20 μM Mg·ATP, and 4 units of inorganic pyrophosphatase (PPiase) in assay buffer. This mixture was assembled directly in a 1 × 1 cm quartz cuvette equipped with a magnetic stir bar. The reaction was initiated by adding a stock solution of DL-4FW prepared in assay buffer to give the desired molar ratios of L-4FW to enzyme dimer concentration. After each addition, the mixture was equilibrated at 25 °C for 4 min. The fluorescence spectrum was then recorded from 305 to 430 nm using an excitation wavelength of 295 nm in a Varian Eclipse fluorimeter (Ontario, Canada). The spectrum for the buffer with 4FW and minus enzyme was subtracted for each corresponding sample spectrum. The integrated fluorescence intensity for each buffer blank-corrected spectrum was determined and plotted against the molar ratio of L-4FW added to TrpRS (dimer).

Titration of TrpRS with 7AW to form 7AW-AMP was performed in assay buffer in a volume of 600 μL using a 0.5 × 0.5 cm cuvette. The reaction was initiated with the addition of a stock solution of DL-7AW, mixing using a Pasteur pipet, and incubating for 10 min at 25 °C prior to recording the fluorescence spectrum from 320 to 450 nm using an excitation wavelength of 310 nm. Each spectrum was buffer blank-subtracted as stated previously to correct for the fluorescence of buffer and enzyme. The integrated fluorescence intensity was calculated and plotted as a function of the ratio of L-7AW added to TrpRS (dimer).

L-[5-^{3}H] Trp-AMP Formation Monitored Using a Filter Binding Assay. Activity assays using [5^{3}H] labeled L-Trp were conducted in the following buffer: 10 mM Tris-HCl, 100 mM NaCl, 1 mM DTT, and 1 mM $MgSO_4$, pH 8.0. Several parallel reactions were conducted with varying concentrations of L-[5^{3}H] Trp. A total reaction volume of 100 μL was used and consisted of 0.5 μM *B. stearothermophilus* TrpRS, 100 μM ATP, and 2 units of PPiase in assay buffer. The reaction was initiated with the addition of L-[5^{3}H] Trp. Whatman anion-exchange filter papers (VWR Canlab, Ontario, Canada) were presoaked in the same assay buffer to which had been added 1 mM cold L-Trp. After 30 min incubation at 25 °C, 75 μL of each sample was applied to a filter paper and allowed to air dry. Filters were washed with 20 mL of buffer containing 1 mM cold L-Trp before counting. Results are presented as the average of three trials.

Table 1: Steady-State and Time-Resolved Fluorescence Parameters for *B. stearothermophilus* TrpRS and Single Trp Mutants[a]

B. stearothermophilus samples	λ_{Max} (nm)	Φ[b]	τ_1[c] (ns)	τ_2 (ns)	τ_3 (ns)	α_1	α_2	α_3	F_1	F_2	F_3
TrpRS	338	0.125	5.45	1.64	0.03	0.37	0.11	0.53	0.91	0.08	0.01
W48	349	0.115	5.13	2.41	0.54	0.60	0.24	0.16	0.82	0.15	0.03
W91	328	0.890	6.02	1.97	0.33	0.14	0.54	0.32	0.42	0.53	0.05
W290	339	0.160	5.42	1.39		0.84	0.16		0.95	0.05	

[a] For the time-resolved data, each rotamer lifetime (τ) and its fractional concentration (α) are reported as is there normalized fractional fluorescence (F). The fluorescence decay profile for each sample was fit to a double or triple exponential decay based on criteria outlined in the Materials and Methods. [b] Quantum yields were determined using *N*-acetyltryptophan amide ($\Phi = 0.14$) as a reference. Samples were prepared in 10 mM PIPES, 100 mM NaCl, 1 mM DTT, pH 7.0. Absorbance readings at 295 nm were measured using a 1×5 cm quartz cuvette. [c] Typical errors for the decay parameters were τ_1, τ_2, τ_3, $\pm$ 0.005 and α_1, α_2, α_3, $\pm$ 0.01.

Counting efficiency was determined to be 36% by spotting a known quantity of L-[5^{3}H] Trp onto a filter paper.

Comparison of X-ray Crystal Structures for the Substrate-Free and Substrate-Bound Forms of B. stearothermophilus TrpRS. Using the PDB coordinates for the substrate-free (ref *15*, PDB ID: 1D2R) and substrate-bound (ref *14*, PDB ID: 1I6K) forms of *B. stearothermophilus* TrpRS (EC: 6.1.1.2), a comparison of the structures was made using WebViewer Lite 4.0 (Molecular Simulations Inc., San Diego, CA). Residue specific comparisons are described in the figure captions as well as the specific atom−atom distance measurements made between the Trp indole nitrogen and an atom of the residue suspected of influencing the fluorescence.

RESULTS

Spectroscopic Characterization of B. stearothermophilus TrpRS and Single Trp Mutants. Several milligrams (approximately 2−3 mg/L of culture) of pure soluble protein were obtained for *B. stearothermophilus* TrpRS and for each of the single Trp mutants as determined using the BCA assay. Enzyme purity was judged by SDS−PAGE to be >98% (data not shown). Activity assays for the formation of the first intermediate were conducted using 7AW as a substrate analogue. This is based upon the previous report showing that 7AW and ATP bind to *B. subtilis* to form a tightly bound 7AW-AMP intermediate with a significantly greater quantum yield than free 7AW (*27*). Titration of *B. stearothermophilus* TrpRS with 7AW in the presence of excess ATP resulted in a large increase in the fluorescence of the analogue and a change in the Stokes' shift from 400 to 360 nm. All single Trp mutants proved to be active in the formation of the adenylate using this assay. Far-UV circular dichroism measurements were made on the *B. stearothermophilus* TrpRS and each single Trp mutant. The resulting spectra were superimposable and showed no significant change in signal over the wavelengths measured (data not shown). Therefore, the mutations introduced in the enzyme do not seem to affect the global secondary structure of *B. stearothermophilus* TrpRS.

The emission maximum for *B. stearothermophilus* TrpRS is 338 nm, and its quantum yield is 0.125 (Table 1). This value reflects the low quantum yield of tryptophans at positions 91 and 48. The time-resolved parameters for single Trp mutants are also presented in Table 1. It must first be noted here that the fluorescence decay parameters of each of the tryptophan residues in the single Trp mutants have important differences. The parameters obtained for the fluorescence decay were those that showed random residual plots and a SVR of 1.9−2.0, indicative of a satisfactory fit

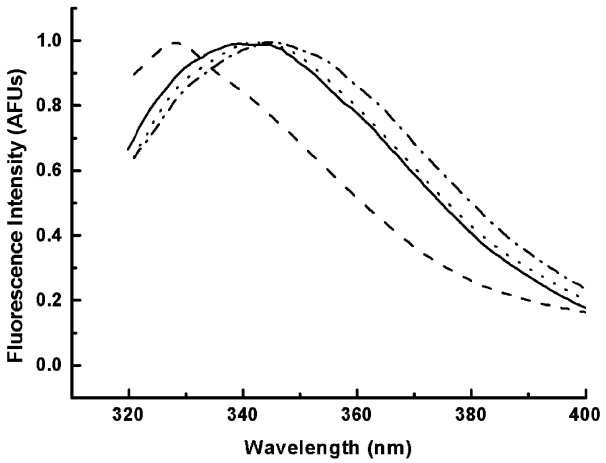

FIGURE 1: Fluorescence emission spectra. For each sample, 1 μM enzyme in 100 mM NaCl, 1 mM DTT, 20 mM Tris-HCl, pH 8.0. (—) *B. stearothermophilus* TrpRS, (— ●) *B. stearothermophilus* W48, (— —) *B. stearothermophilus* W91, and (●) *B. stearothermophilus* W290.

to the data. Fits to data were also judged to be adequate when random distribution in the residual plots was observed. There are three distinct decay times visible in its fluorescence decay profile of *B. stearothermophilus* TrpRS, and the overall fluorescence is dominated by the longest and shortest components with preexponential terms of 0.37 and 0.53, respectively. The fluorescence spectrum of the single Trp residue in each mutant varied with *B. stearothermophilus* W91 having the shortest wavelength maximum at 328 nm (Figure 1). This reflects the hydrophobic environment at the dimer interface. The quantum yield of Trp in this mutant was 0.089. Both *B. stearothermophilus* W48 and *B. stearothermophilus* W290 displayed broader spectral profiles and a red-shifted fluorescence spectrum with maxima at 349 and 339 nm, respectively. The corresponding quantum yields were 0.12 and 0.16. The average quantum yield of the three mutants is 0.121, which is very similar to the value of 0.125 obtained for the nonmutated enzyme. The fluorescence decay of *B. stearothermophilus* W91 was best described by a three exponential fit. It displayed the longest lifetime for any of the mutants with a value of 6.02 ns. The preexponential term for a decay component is proportional to the relative concentration of that component (*33*). The preexponential terms for this mutant were significantly different from those of other mutants with values of 0.14, 0.54, and 0.32 for the long, medium, and short decay time components, respectively. The fluorescence is dominated by the second decay component with a lifetime of 2.41 ns. There are only two decay times associated with Trp 290 fluorescence with

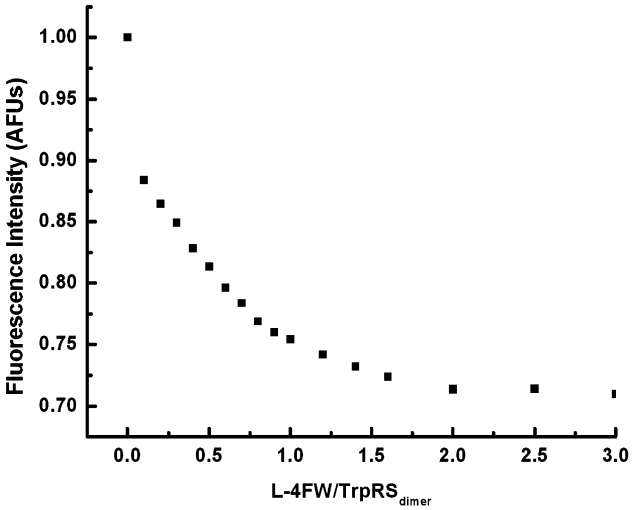

FIGURE 2: Formation of 4FW-AMP in *B. stearothermophilus* TrpRS. Intrinsic fluorescence emission monitored with 295 nm excitation, after incubating L-4FW in the presence of 1 μM enzyme and 20 μM ATP at pH 8.0.

lifetimes of 5.42 and 1.39 ns. The fluorescence is dominated by the long lifetime component, which has a normalized preexponential term of 0.84. *B. stearothermophilus* W48 also displayed three distinct lifetimes of 5.13, 2.41, and 0.54 ns. The fluorescence of the long lifetime component made the largest contribution to the fluorescence.

Substrate Titrations Forming the Aminoacyl-AMP Intermediate. All reactions contained inorganic pyrophosphatase and excess ATP to drive the reaction forward to completion; therefore, a true equilibrium was never established. The fluorescence of *B. stearothermophilus* TrpRS reflects the contribution of each intrinsic Trp. Upon forming the 4FW-AMP intermediate, there is a decrease in fluorescence of 27% (Figure 2). This quenching reaches a plateau after a 1:1 4FW to TrpRS dimer ratio had been reached. Titration of each enzyme mutant with 4FW to form 4FW-AMP resulted in significant changes in the intrinsic Trp fluorescence. Control reactions in which ATP or 4FW were omitted resulted in no change in fluorescence, suggesting that the observed changes are the result of 4FW-AMP formation. In each case, the majority of the observed fluorescence change was complete after 1 mol equiv (to the TrpRS dimer) of L-4FW was added. This corresponds with the formation of one intermediate molecule per molecule of dimer. *B. stearothermophilus* W91 displayed the largest change in signal upon titration with a decrease in fluorescence intensity of 49% (Figure 3A). Previous work showed a similar quenching of the analogous Trp 92 at the dimer interface (*22*). It was suggested at the time that a nearby cysteine residue (Cys 95) may be the quenching group. To test this, the cysteine to serine mutant was constructed. The fluorescence of *B. subtilis* C96S decreased 62% upon titration with 4FW (Figure 4), which is similar to that observed in the *B. stearothermophilus* TrpRS. *B. stearothermophilus* W290 showed a quenching of fluorescence of 22% (Figure 3B). *B. stearothermophilus* W48 displayed an increase (19%) in fluorescence (Figure 3C) with no change in emission maximum. In each of the previous titrations, there was negligible change in fluorescence beyond a 1:1 ratio.

Monitoring the absorbance changes in the enzyme at 290 nm provided another means of measuring structural changes

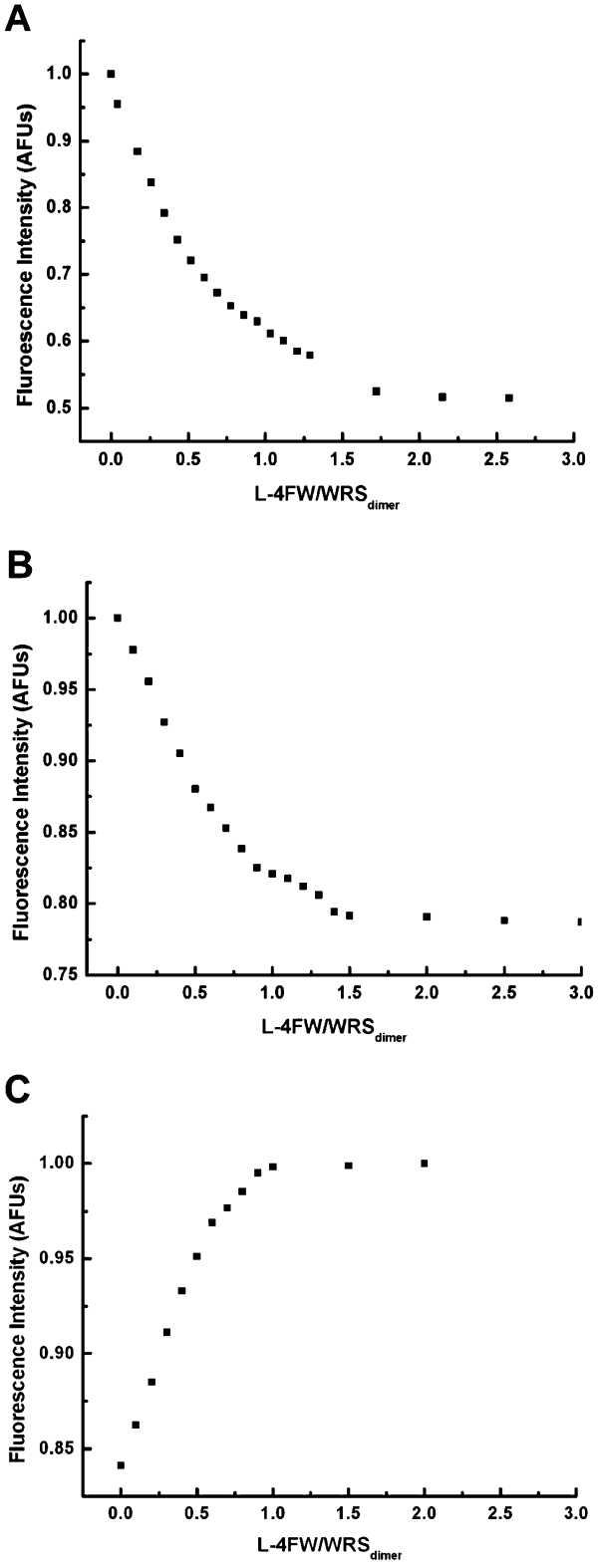

FIGURE 3: Formation of 4FW-AMP in single Trp mutants. Intrinsic fluorescence emission monitored with 295 nm excitation, after incubating L-4FW in the presence of 1 μM enzyme and 20 μM ATP at pH 8.0. (A) *B. stearothermophilus* W91. (B) *B. stearothermophilus* W290. (C) *B. stearothermophilus* W48.

in the protein upon titration with an analogue. Using 4FW, the observed signal change was correlated with Trp and tyrosine residues since the extinction coefficient for this analogue is low at 290 nm. The absorbance changes upon forming 4FW-AMP are shown in Figure 5. For each point,

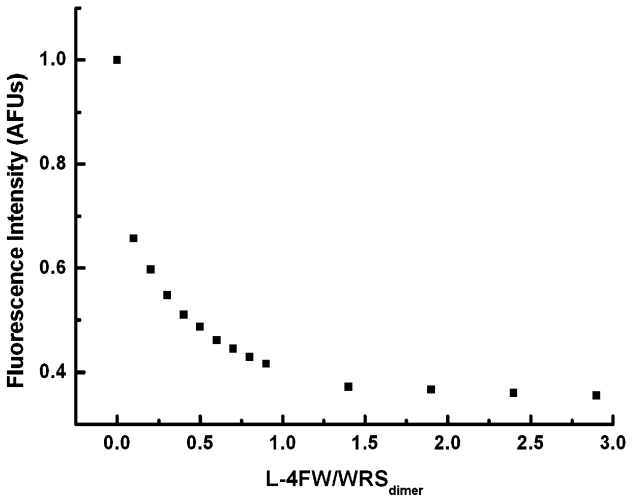

FIGURE 4: Formation of 4FW-AMP in the *B. subtilis* C96S single Trp mutant. Intrinsic fluorescence emission was monitored using 295 nm excitation after incubating L-4FW in the presence of 1 μM enzyme and 20 μM ATP at pH 8.0.

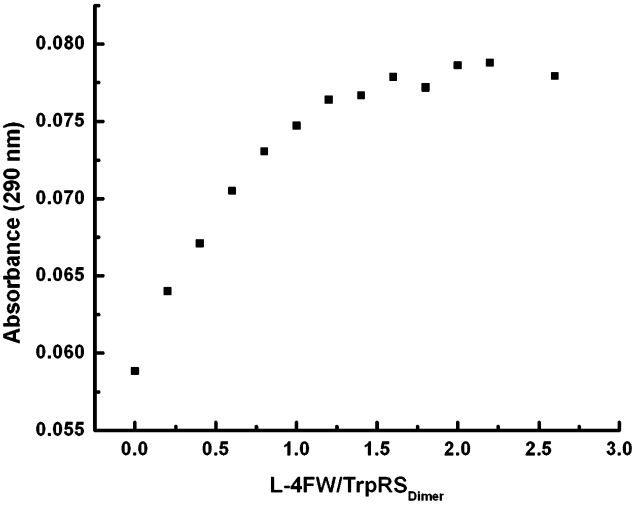

FIGURE 5: Absorbance changes upon forming 4FW-AMP in *B. stearothermophilus* W91 mutant. The absorbance at 290 nm was monitored after incubation of various concentrations of L-4FW in the presence of 2 μM enzyme and 40 μM ATP at pH 8.0.

the absorbance of buffer with ATP has been subtracted; therefore, the observed signal change is that of the Tyr and Trp residues in the enzyme. It shows a pattern similar to that observed with fluorescence measurements in that the bulk of the signal change (increase in absorbance) was observed with the formation of 1 equiv of 4FW-AMP. The results of the titration of W91 with 7AW in the presence of ATP to form the 7AW-AMP intermediate are shown in Figure 6. As with the 4FW reaction, the majority of the fluorescence change was observed after the addition of one mole equivalent of L-7AW to the dimeric enzyme. In the presence of inorganic pyrophosphatase, all 7AW added to the solution should be bound to AMP in the active site up to a 1:1 ratio. Therefore, no correction for free 7AW is necessary. Beyond this 1:1 ratio, a correction was made by subtracting the fluorescence contribution of an equivalent quantity of free 7AW titrated into a buffer solution. Despite this correction, there was a small but consistent increase in 7AW fluorescence intensity beyond the 1:1 ratio. The results

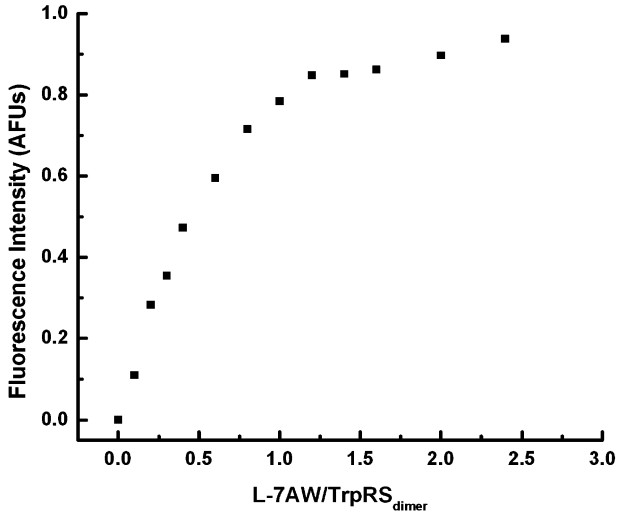

FIGURE 6: 7AW titration of *B. stearothermophilus* W91 single Trp mutant. Fluorescence of the Trp analogue was monitored exclusively using 315 nm excitation. The emission spectrum from 320 to 450 nm was recorded, and the integrated fluorescence intensity of each curve was plotted against the ratio of analogue to enzyme dimer. Reaction conditions were 1 μM enzyme and 20 μM ATP at pH 8.0. Beyond a 1:1 ratio, the data were corrected for the fluorescence of free 7AW by subtracting the appropriate blank solution.

from the reactions forming the aminoacyl-AMP intermediate suggest that only one of the two reactive sites of the homodimer is filled with 4FW-AMP or 7AW-AMP, respectively, when stoichiometric concentrations of amino acid are used. While the fluorescence and absorption experiments with 4FW all strongly indicate that only one of the two reactive sites of the homodimer is filled with substrate, there existed the possibility that the second site might also fill but not result in any change in observed signal. For 7AW, the small increase in fluorescence beyond 1:1 suggests some binding to the second subunit albeit with a lower affinity. The rationale for this is that the structure of the dimer is symmetrical when both subunits are filled with Trp-AMP; therefore, the observed fluorescence changes for each substrate should be equivalent. The high sensitivity of 7AW fluorescence to exposure to solvent suggests that it is unlikely that binding of the analogue to the second free subunit would not cause a change in its fluorescence signal. To better interpret these results, a direct quantitative measurement of bound Trp-AMP, under conditions similar to those used in the analogue-AMP reactions, was conducted using L-(5^3H) Trp in an ion-exchange filter binding assay. The experiment involved incubation of solutions containing different concentrations of L-[5^3H] Trp in the reaction buffer. The reaction mixture was passed over an anion-exchange filter, which trapped the enzyme together with any Trp-AMP bound in the active site(s). The data for this experiment are presented in Figure 7. The results are consistent with the formation of 1 mol equiv of Trp-AMP to enzyme dimer. This confirms that under the nonsaturating conditions used here, the Trp-AMP activity of the second subunit is inhibited or reduced significantly. These results are similar to those observed for *B. subtilis* TrpRS (i.e., one reactive subunit) but differ from those for TrpRS isolated from bovine pancreas, which forms 2 equiv of Trp per dimer under similar conditions to those stated previously (*21*).

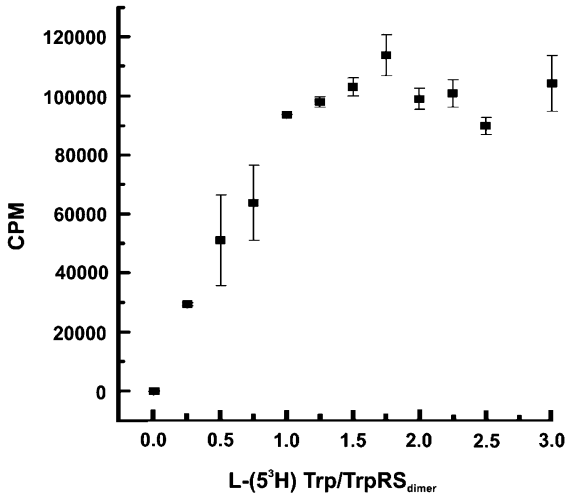

FIGURE 7: Formation of Trp-AMP in *B. stearothermophilus* TrpRS monitored using radiolabeled substrate. L-[5-^{3}H] Trp was titrated into samples of enzyme with ATP and PPiase in assay buffer and incubated at 25 °C for 15 min prior to spotting onto anion-exchange filter papers. These were then dried and washed extensively prior to counting. Results are presented as the mean of three trials.

DISCUSSION

Spectroscopic analysis of single Trp mutants of *B. stearothermophilus* TrpRS has provided new details of the movements within different segments of the enzyme during the first step of the enzymatic reaction. Together with the recent publication of the X-ray crystal structure for the substrate-free form of *B. stearothermophilus* TrpRS and the substrate-bound structure reported previously, this gives a detailed view of the enzyme prior to and after forming Trp-AMP. The fluorescence observations made during Trp-AMP formation with each single Trp mutant show that significant structural changes occur throughout the subunit that forms the adenylate ester and that these changes are not limited to the active site or dimer interface. This had been suggested in the static X-ray crystal structural data (*14*, *15*). Fluorescence measurements upon forming 4FW-AMP could be attributed to structural changes occurring at each Trp position. The fluorescence of both W91 and W290 was quenched during the formation of 4 FW-AMP. In each case, there was no change in emission maximum indicating that there was negligible change in polarity of the Trp environment, such as increased solvent exposure. For *B. subtilis* TrpRS, a large quenching (>70%) of the fluorescence of the single Trp residue at position 92 had been reported upon formation of the Trp-AMP intermediate (*22*). This change was suggested to be due to a rearrangement from a coil to helix conformation in the segment containing the Trp. Being four residues away, this could position the Cys 96 residue in an adjacent orientation to the Trp indole ring that would be the origin of the quenching of Trp fluorescence. However, according to the crystal structures, there is less than a 0.3 Å change in distance between the sulfur atom of Cys 95 and the N1 indole nitrogen of Trp91 for *B. stearothermophilus* TrpRS in going from substrate-free to Trp-AMP-bound forms (Figure 8A). To test the original hypothesis, the C96S mutant of *B. subtilis* TrpRS was constructed and expressed. 4FW-AMP formation in the C96S mutant resulted in 62% quenching in fluorescence. This was comparable to the observed quenching with the Cys residue in place, and we now believe that Cys 96 is

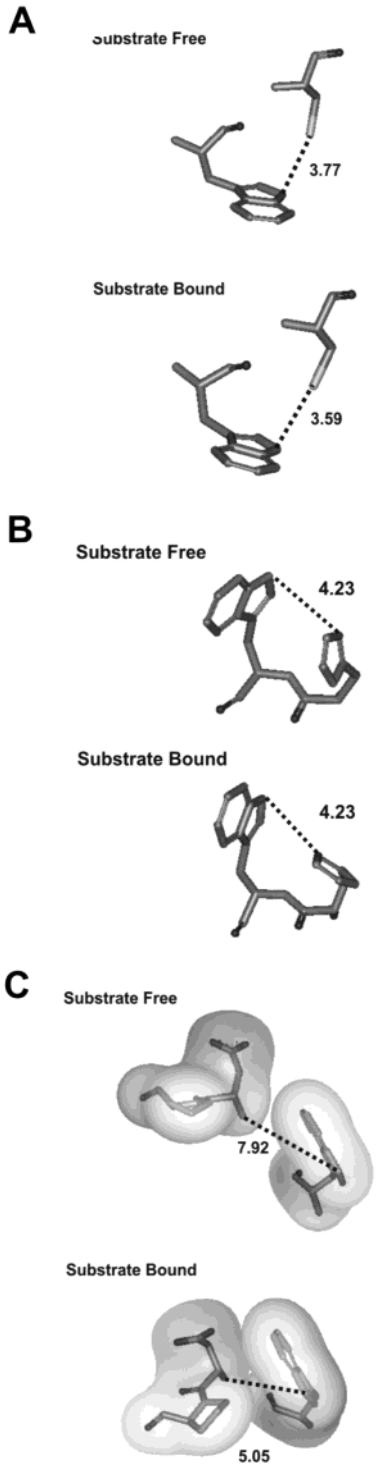

FIGURE 8: Comparison of X-ray crystal structures. (A) Change in position of the sulfur atom of the Cys95 quenching group relative to indole nitrogen of Trp 91 in *B. stearothermophilus* TrpRS. There is a decrease in distance between the two atoms of 0.3 Å. (B) Change in position of the C1 atom of the His 289 imidazole ring relative to the indole nitrogen of Trp 91 in *B. stearothermophilus* TrpRS. The imidazole ring goes from an approximately parallel to perpendicular orientation relative to the indole ring without a significant change in distance. (C) Change in position of the backbone nitrogen atom of Asp 50 relative to indole nitrogen of Trp 48 in *B. stearothermophilus* TrpRS. One face of the indole ring approaches Asp 50 and Pro 51, shielding it from solvent. The structures of both the substrate-free (*15*) and substrate-bound forms (*14*) of the enzyme are shown.

not responsible for the bulk of the observed quenching of the Trp 92 residue. There is consistent evidence that multicomponent fluorescence decay curves can be attributed to the presence of side chain rotamers of this amino acid (*33*). Thus, the preexponential terms of the fluorescence decay parameters are proportional to the relative population of these rotamers. The time-resolved data indicated that the favored rotamer conformation of the Trp indole ring at position 91 was not the one that had the longest fluorescence decay time. A similar observation was made for *B. subtilis* TrpRS (*22*). This previous report also showed that upon forming the adenylate intermediate, there was a shift in rotamer populations of Trp 92. The fluorescence decay of the adenylate intermediate-bound form of the enzyme was dominated by the shortest decay component in this case as well. This provides an explanation for the large quenching of fluorescence observed in both TrpRS enzymes. The results can be rationalized by a redistribution of the rotamer population on forming the Trp-adenylate where the rotamer having the indole ring located adjacent or closest to the amide backbone becomes the dominant conformation. It has been reported that such a rotamer would result in the quenching of Trp fluorescence owing to the increased probability of excited-state electron transfer to the carbonyl group of the amide backbone (*35*). The X-ray crystal structures of *B. stearothermophilus* TrpRS show that Trp 91 is situated in an α-helix with or without Trp-AMP. The crystal structures of the substrate-free enzyme and the symmetric dimer structure of the adenylate-bound form do not permit a rationalization of the observed fluorescence changes. If the 1:1 adenylate/dimer complex is asymmetric and affects the dimer interface, then the time-resolved fluorescence data of *B. stearothermophilus* W91 may provide insights into the changes in indole side chain conformations that occur.

A structural change at position 290, inferred from the quenching of the fluorescence of the Trp residue at this position upon formation of the adenylate ester, is significant given the distance of W290 from both the Trp-AMP (23 Å) and the tRNA binding sites (19 Å) (*14*). As with the data from position 91, the fluorescence results from position 290 show that structural changes are not limited to the active site. There is a lack of any significant change in solvent exposure of the indole ring of Trp 290 between the substrate-free and the bound forms as demonstrated by the similarity in fluorescence maxima. This agrees with the information provided by X-ray structures. The only residue within a 6 Å distance of the indole moiety at this position that would be capable of quenching W290 fluorescence is His 289. In the substrate-bound form, the plane of the imidazole ring of the His residue has rotated from a configuration where the two ring structures were parallel to one where the imidazole ring is perpendicular to the plane of the indole ring of Trp (Figure 8B). The parallel orientation is the dominant configuration found between these two ring structures in proteins (*36*). The relative change in distance between the two functional groups was negligible, and that alone cannot explain the observed quenching. However, the change in ring orientation when forming Trp-AMP may lead to a more efficient proton-transfer quenching process from His 289 to Trp 290 (*37*). The double exponential time-resolved florescence decay parameters also support the idea of reduced conformational freedom for the indole ring.

Previous experiments have suggested that there are changes occurring in the substrate-free subunit when one subunit formed the adenylate. This came from the observation of fluorescence changes occurring at the dimer interface when forming the intermediate (*22*). The method for inter-subunit communication has not been established, although movement in the long helical backbone, containing Trp 290, has been suggested as one possibility (*15*). The C-terminal end of this backbone inserts into the dimer interface, making contact with residues in the other subunit. The flexibility of this helical axis implied by the observed fluorescence changes supports the idea that upon forming the first intermediate, there is a structural change in the reactive subunit that induces a similar structural change in the second substrate-free subunit via the dimer interface.

Trp 48 is located on the opposite face of the active site with the indole ring oriented away from the surface of the enzyme. Given its solvent-exposed nature and distance from the active site (22 Å), it was not expected to show any changes in fluorescence upon forming the ester intermediate. The indole ring of Trp 48 is fully solvent exposed on both faces in the substrate-free form (Figure 8C). In the substrate-bound form of the enzyme, there is a conformational change in this segment that brings one face of the indole ring in contact with Asp 50 and Pro 51, shielding it from solvent. This partial shielding from solvent quenching could explain the observed increase in fluorescence.

Titration of TrpRS with 7AW to form 7AW-AMP resulted in a large increase in 7AW fluorescence after approximately 1 mol equiv of 7AW had been added. Further titration with this analogue resulted in a much smaller increase in intensity up to and beyond a 2:1 complex. The X-ray crystal structure for *B. stearothermophilus* TrpRS with both subunits filled with Trp adenylate is symmetrical. If both sites were forming 7AW-AMP with equal efficiencies then one expects twice the observed increase in 7AW fluorescence at saturation. If the second subunit has a different structure when filled, then the observed signal change should reach saturation at a 2:1 ratio since in this reaction one is monitoring the change in signal of the reacting amino acid substrate and not that of enzyme itself. This anti-cooperative behavior implies that the formation of the complex at one active site and the concomitant structural changes in that subunit induce a structural changes in the second subunit that prevent the efficient formation of a second adenylate moiety in the dimer. This possibility is seen from the symmetrical structures as discussed earlier. This suggests that the affinity for 7AW and/or the catalytic efficiency in forming 7AW-AMP is significantly reduced at the second substrate-free subunit. It is reasonable to assume, given these results, that binding of 4FW, or formation of 4FW-AMP, may also occur at the second substrate-free subunit in the analogous titration. It should be pointed out, however, that no further changes in the fluorescence of any of *B. stearothermophilus* TrpRS or any of the single Trp mutants were observed beyond a 1:1 TrpRS:4FW-AMP complex. This pattern in stoichiometry was also observed in the experiments measuring absorbance during the formation of 4FW-AMP. The radioisotope assay shows clearly that there is no significant formation of Trp-AMP after forming the intermediate at one subunit. Together with the spectroscopic data, this indicates an anticooperative model. It should be noted that since inorganic pyrophos-

phatase has been added to each reaction mixture, this eliminates the possibility of complex inhibition by bound pyrophosphate. Bound pyrophosphate had been proposed previously as an explanation for the anticooperative behavior observed in bovine TrpRS (*21*).

The results from the 4FW-AMP reaction suggest that (1) there are major structural changes occurring in both subunits after forming a 1:1 complex and (2) it is unlikely that additional changes in structure occur upon the filling of the second subunit. These results suggest that an approaching $tRNA^{Trp}$ molecule will likely bind to a dimeric enzyme that has one subunit filled. In the acylation reaction, the anticodon region of the tRNA will make contact with the substrate-free subunit, spanning the dimer so that the 3′ end is close to the filled active site. Therefore, the structure presented in the X-ray crystal data, in which both subunits are filled, is likely to be very similar to that encountered by the approaching $tRNA^{Trp}$ in solution under nonsaturating conditions, where only one subunit is occupied. If both subunits share a similar structure, an approaching tRNA molecule could bind to the enzyme in an orientation that would not result in amino acid acetylation. Further experiments are required to determine if an approaching tRNA molecule has any preference to the subunit carrying the Trp-AMP intermediate.

CONCLUSIONS

The data from the single Trp mutants demonstrate the utility of intrinsic fluorescence as a method for providing new insights into structure−function relationships in highly dynamic proteins as well as complementing the data available from X-ray structures. The binding of Trp and ATP in *B. stearothermophilus* TrpRS to form Trp-AMP results in a global change in structure at the active subunit. These changes are communicated to the second substrate-free subunit, where it is believed that a similar structure is induced. The mechanism for this communication may be through movement in the long helical backbone via the dimer interface. Under physiological nonsaturating conditions, the second subunit does not form Trp-AMP, which was shown to be the case in the X-ray crystal structure where saturating concentrations of substrate were used in producing the crystals for diffraction. The structure of the empty subunit is believed to be that observed in the substrate-filled active subunit shown in X-ray crystal structure data, where an excess of substrates were used since the active site of the second subunit does not efficiently form adenylate. This differs from the enzyme preparation used for generating the X-ray crystal structure where saturating concentrations of substrate were used. This change in structure of the free subunit may explain the observed anticooperativity.

ACKNOWLEDGMENT

We would like to thank Dr. Sandy Ross (Department of Chemistry, University of Montana) for providing time-resolved fluorescence data on the *B. stearothermophilus* W48 mutant.

REFERENCES

1. Ibba, M., and Soll, D. (2000) *Annu. Rev. Biochem. 69*, 617.
2. Arnez, J., and Moras, D. (1997) *Trends Biochem. Sci. 22*, 211.
3. Schimmel, P. (1987) *Annu. Rev. Biochem. 56*, 125.
4. Delarue, M. (1995) *Curr. Opin. Struct. Biol. 5*, 48.
5. Cusack, S. (1997) *Curr. Opin. Struct. Biol. 7*, 881.
6. Guo, Q., Gong, Q., Tong, K., Vestergaard, B., Costa, A., Desgres, J., Mansim, W., Grosjean, H., Zhu, G., Wong, T., and Xue, H. (2002) *J. Biol. Chem. 277*, 14343.
7. Eriani, G., Delarue, M., Pock, O., Gangloff, J., and Moras, D. (1990) *Nature 347*, 203.
8. Burbaum, J., and Schimmel, P. (1991) *J. Biol. Chem. 266*, 16965.
9. Schimmel, P., Tao, J., and Hill, J. (1998) *FASEB J. 12*, 1599.
10. Martinis, S. A., Plateau, P., Cavarelli, J., and Florentz, C. (1999) *EMBO J. 18*, 4591.
11. Dorizzi, M., Labouesse, B., and Labouesse, J. (1971) *Eur. J. Biochem. 19*, 563.
12. Dorizzi, M., Labouesse, B., and Labouesse, J. (1971) *Eur. J. Biochem. 19*, 81.
13. Dorizzi, M., Merault, G., Fournier, M., Labouesse, J., Keith, G., Dirheimer, G., and Buchingham, R. (1977) *Nucleic Acids Res. 4*, 31.
14. Doublie, S., Bricogne, G., Gilmore, C., and Carter, C. W., Jr. (1995) *Structure 3*, 17.
15. Ilyin, V. A., Temple, B., Mei, J., Genpei, L., Yuhui, Y., Patrice, V., and Carter, C. W., Jr. (2000) *Protein Sci. 9*, 218.
16. Mazat, J. P., Merle, M., Graves, P. V., Merault, G., Gandar, J. C., and Labouesse, B. (1982) *Eur. J. Biochem. 128*, 389.
17. Ward, W. H., and Ferst, A. R. (1988) *Biochemistry 27*, 5525.
18. Rould, M., Perona, J., Soll, D., and Steitz, T. (1989) *Science 246*, 1135.
19. Biou, V., Yaremchuk, A., Tukalo, M., and Cusack, S. (1994) *Science 263*, 1404.
20. Fersht, A. R., Ashford, J. S., Bruton, C. J., Jakes, R., Koch, G. L., and Harley, B. S. (1975) *Biochemistry 14*, 1.
21. Degtyarev, S. K., Beresten, S. F., Denisov, A. Y., Lavrik, O. L., and Kisselev, L. L. (1982) *FEBS Lett. 137*, 95.
22. Hogue, C. W., Doublie, S., Xue, H., Wong, J. T., Carter, C. W., Jr., and Szabo, A. G. (1996) *J. Mol. Biol. 260*, 446.
23. Fournier, M., Plantard, C., Labouesse, B., and Labouesse, J. (1987) *Biochim. Biophys. Acta 916*, 350.
24. Sever, S., Rogers, K., Rojers, M. J., Carter, C. W., Jr., and Soll, D. (1996) *Biochemistry 35*, 32.
25. Chow, K., Xue, H., Shi, W., and Wong, J. (1992) *J. Biol. Chem. 267*, 9146.
26. Graves, P. V., Bony, J., Mazat, J. P., and Labouesse, B. (1980) *Biochimie 62*, 33.
27. Hogue, C. W., and Szabo, A. G. (1993) *Biophys. Chem. 48*, 159.
28. Nevinsky, G. A., Favorova, O. O., Lavrik, O. I., Petrova, T. D., Kochikina, L. L., and Savchenko, T. I. (1974) *FEBS Lett. 43*, 135.
29. Xu, Z. J., Love, M. L., Ma, L. Y., Blum, M., Bronskill, P. M., Berstein, J., Grey, A. A., Hofmann, T., Cameran, N. and Wong, J. T. (1989) *J. Biol. Chem. 264*, 4304.
30. Ross, J. B., Szabo, A. G., and Hogue, C. W. (1997) *Methods Enzymol. 278*, 151.
31. Brennan, J. D., Hogue, C. W., Rajendran, B., Willis, K. J., and Szabo, A. G. (1997) *Anal. Biochem. 252*, 260.
32. Lett, C. M., Rosu-Myles, M. D., Frey, H. E., and Guillemette, J. G. (1999) *Biochim. Biophys. Acta 1432*, 40.
33. Dahms, T. E., Willis, K. J., and Szabo, A. G. (1995) *J. Am. Chem. Soc. 117*, 2321.
34. Smith, P. K., Krohn, R. I., Hermanson, G. T., Mallia, A. K., Gartner, F. H., Provenzano, M. D., Fujimoto, E. K., Goeke, N. M., Olson, B. J., and Klenk, D. C. (1985) *Anal. Biochem. 150*, 76.
35. Adams, P. D., Chen, Y., Ma, K., Zagorski, M. G., Sonnichsen, F. D., McLaughlin, M. L., and Barkley, M. D. (2002) *J. Am. Chem. Soc. 124*, 9278.
36. Samanta, U., Pal, D., and Chakrabarti, P. (1999) *Act. Crystallogr., Sect. D 55*, 1421.
37. Szabo, A. G. (1989) The fluorescence properties of aromatic amino acids: Their role in the understanding of enzyme structure and dynamics, in *The Enzyme Catalysis Process* (Cooper, A., and Chien, L. C., Eds.) pp 123−140, Plenum Press, New York.

BI0347454